JACC: CARDIOVASCULAR IMAGING
VOL. 8, NO. 1, 2015

ISSN 1936-878X/$36.00
PUBLISHED BY ELSEVIER INC.
http://dx.doi.org/10.1016/j.jcmg.2014.09.018

^{11}C-Pittsburgh B PET Imaging in Cardiac Amyloidosis

Seung-Pyo Lee, MD, PhD,*† Eun Seong Lee, MD,‡ Hongyoon Choi, MD,‡ Hyung-Jun Im, MD,‡ Youngil Koh, MD,† Min-Ho Lee, MD,*† Ji-Hyun Kwon, MD,† Jin Chul Paeng, MD, PhD,‡ Hyung-Kwan Kim, MD, PhD,*† Gi Jeong Cheon, MD, PhD,‡ Yong-Jin Kim, MD, PhD,*† Inho Kim, MD, PhD,† Sung-Soo Yoon, MD, PhD,† Jeong-Wook Seo, MD, PhD,§ Dae-Won Sohn, MD, PhD*†

ABSTRACT

OBJECTIVES This study sought to investigate the efficacy of ^{11}C-Pittsburgh B (PiB) positron emission tomography (PET)/computed tomography (CT) in the diagnosis of cardiac amyloidosis.

BACKGROUND The PiB compound has been promising for detection of amyloid deposits in the brain.

METHODS A total of 22 consecutive patients were enrolled in this prospective pilot study of monoclonal gammopathy patients with suspected cardiac amyloidosis. The study consisted of a series of ^{11}C-PiB PET/CT, echocardiography, cardiac magnetic resonance, and endomyocardial biopsy within a 1-month period. In addition, 10 normal subjects were recruited to determine the most optimal cut-off value for a positive ^{11}C-PiB PET/CT scan.

RESULTS Among the 22 patients, 15 patients were diagnosed as cardiac amyloidosis by endomyocardial biopsy and 5 patients had undergone chemotherapy previously before the ^{11}C-PiB PET/CT. There were no differences in echocardiographic parameters between patients with versus without cardiac amyloidosis, except for a marginal difference in the left ventricular end-diastolic dimension (median 41.0 mm [range 33.0 to 49.0 mm] vs. 50.0 mm [range 38.0 to 55.0 mm], $p = 0.066$). ^{11}C-PiB PET/CT was positive in 13 of 15 biopsy-proven cardiac amyloidosis patients, whereas none of the patients without cardiac amyloidosis demonstrated positive ^{11}C-PiB PET/CT scan results. The maximal myocardium-to-blood cavity ratio was significantly different between patients with versus without cardiac amyloidosis (median 3.9 [range 1.7 to 19.9] vs. 1.0 [range 0.8 to 1.2], $p < 0.001$). In association with the significant difference of ^{11}C-PiB uptake in the myocardium between the chemotherapy naïve versus the previous chemotherapy group (median 10.4 [range 1.7 to 19.9] vs. 2.3 [range 1.7 to 3.8], $p = 0.014$), all except 1 patient among the 5 previously treated patients had responded to chemotherapy by serum free light chain assay results at the time of ^{11}C-PiB PET/CT scan.

CONCLUSIONS ^{11}C-PiB PET/CT may be valuable for the diagnosis of cardiac amyloidosis noninvasively. Whether ^{11}C-PiB PET/CT may be a good surrogate marker of active light chain deposition in the myocardium warrants further investigation in a larger number of patients. (J Am Coll Cardiol Img 2015;8:50–9) © 2015 by the American College of Cardiology Foundation.

Cardiac amyloidosis is characterized by diffuse, patchy extracellular infiltration of the myocardium with water-insoluble fibrillary proteins (1,2). In an advanced stage, cardiac amyloidosis is usually manifested as restrictive cardiomyopathy, the clinical management of which is challenging and the prognosis of which is extremely dismal (3,4).

From the *Cardiovascular Center, Seoul National University Hospital, Seoul, Korea; †Department of Internal Medicine, Seoul National University College of Medicine, Seoul National University, Seoul, Korea; ‡Department of Nuclear Medicine, Seoul National University Hospital and Seoul National University College of Medicine, Seoul, Korea; and the §Department of Pathology, Seoul National University Hospital and Seoul National University College of Medicine, Seoul, Korea. This study was supported by a grant from the Korean Health Technology R&D Project funded by the Ministry of Health, Welfare & Family Affairs (A120753). All authors have reported that they have no relationships relevant to the contents of this paper to disclose.

Manuscript received April 9, 2014; revised manuscript received September 15, 2014, accepted September 22, 2014.

Although the gold standard for the diagnosis of cardiac amyloidosis is tissue confirmation by endomyocardial biopsy (5), this technique is invasive and may be avoided if the presence of amyloid deposit is confirmed by histology in another organ and cardiac amyloidosis can be diagnosed on the basis of noninvasive findings suggestive of cardiac involvement. In addition, biopsy of a focal myocardium may not provide information about the amyloidogenic protein burden in the whole myocardium, nor does it give information on whether the protein accumulation is active.

SEE PAGE 60

Therefore, there is a clinical need for accurate assessment of cardiac amyloidosis noninvasively. Moreover, a method that can give a quantitative estimate of amyloid deposit may also provide us with clinically important information regarding the prognosis. The Pittsburgh B (PiB) compound, a derivative of thioflavin-T, has been used with very good results for imaging β-amyloid in Alzheimer's disease (6) and is believed to bind to amyloid fibril of any type (7).

We expected positron emission tomography (PET) imaging using this compound to be a promising choice for imaging cardiac amyloidosis, the preliminary results of which has been successful in a small case series (8). In this pilot study, we present the analysis results of a prospective cohort of cardiac amyloidosis patients examined using the ^{11}C-PiB PET/computed tomography (CT) scan, together with cardiac magnetic resonance (CMR), echocardiography, and endomyocardial biopsy.

METHODS

A detailed version of the Methods section is described in the Online Appendix.

PATIENT POPULATION. A total of 27 patients were consecutively assessed for eligibility to this prospective study from January 2012 to October 2013, which consisted of a series of ^{11}C-PiB PET/CT, CMR, echocardiography, endomyocardial biopsy, and laboratory tests such as free light chain assay for monoclonal gammopathy. The patients were enrolled in this study if they had serum monoclonal gammopathy plus any of the following criteria (5):

1. Average left ventricular (LV) thickness ≥11 mm on echocardiography in the absence of uncontrolled hypertension;
2. Unexplained low voltage <0.5 mV in the limb leads of the 12-lead electrocardiogram; or
3. Biopsy-proven amyloidosis in any other organ.

Among the 27 patients, 2 patients refused endomyocardial biopsy, 2 patients refused to take ^{11}C-PiB PET/CT despite endomyocardial biopsy, and 1 patient refused both ^{11}C-PiB PET/CT and endomyocardial biopsy. Therefore, the final target population for this analysis was 22 patients. This study was conducted according to the principles outlined in the Declaration of Helsinki. All patients gave written informed consent to this prospective study, the protocol of which was approved by the Institutional Review Board of Seoul National University Hospital. The ^{11}C-PiB PET/CT, CMR, echocardiography, and endomyocardial biopsy were completed within 1 month of enrollment. All except 1 patient, who had a history of coronary revascularization for a single-vessel disease, were void of any history of significant coronary artery disease. In addition, all patients denied any history of myocardial infarction, which was also confirmed by the late gadolinium enhancement (LGE) pattern in CMR. The patients were divided into a cardiac amyloidosis group versus no cardiac amyloidosis group, according to the endomyocardial biopsy results, and the cardiac amyloidosis group was divided further into a chemotherapy naïve group versus the previous chemotherapy group according to whether the patient had undergone previous chemotherapy before the ^{11}C-PiB PET/CT scan.

In addition, we enrolled 10 normal subjects (4 males, age range 37 to 80 years) without any evidence of heart disease to determine the cut-off value of the positive ^{11}C-PiB PET/CT scan.

^{11}C-PIB PET/CT SCAN AND ANALYSIS OF PET RESULTS. After low-dose CT scanning, 555 MBq of ^{11}C-PiB was injected through the antecubital vein, followed by an emission scan 30 min after the tracer injection using a PET/CT scanner with a spatial resolution of 4.2 mm (Biograph 40, Siemens Medical Solutions, Knoxville, Tennessee). Imaging was performed in 3-dimensional mode for 3 min per bed position after 30 min of tracer injection. All appropriate corrections for scanner normalization, dead time, decay, scatter, randoms, and attenuation were applied. Images were reconstructed on 256 × 256 matrices using an ordered-subset expectation maximization method (4 iterations, 8 subsets) with the application of a 5-mm Gaussian filter. Images were displayed on transaxial, coronal, and sagittal planes of 5-mm slice thickness.

The standard uptake value (SUV) of the myocardium was measured by drawing the contour of the whole LV at an approximate thickness of 10 mm

ABBREVIATIONS AND ACRONYMS

CMR = cardiac magnetic resonance
CT = computed tomography
LGE = late gadolinium enhancement
LV = left ventricle/ventricular
PET = positron emission tomography
PiB = Pittsburgh B
RV = right ventricle/ventricular
SUV = standard uptake value

from the base to apex. The maximal SUV was defined as the maximal SUV in all of the volume of interest (VOIs) analyzed. The mean SUV was defined as the mean SUV of the total voxels in the VOI. The maximal/mean myocardium to blood cavity ratio was defined as the maximal/mean SUV of the myocardial VOI divided by the mean SUV of the descending thoracic aorta VOI. The mean SUV of the right ventricle (RV) was analyzed in a similar manner from the RV free wall.

To determine the optimal cut-off value of ^{11}C-PiB PET/CT, we analyzed the images of 10 sex-matched normal subjects (Table 1). As the amyloid protein deposit may be heterogeneous (9), the cut-off value was determined with the maximal rather than the mean LV myocardium to blood cavity ratio. The maximal LV myocardium to blood cavity ratio did not exceed 1.6 in all control subjects. In addition, 2 weeks later, intraobserver variability of the maximal LV myocardium to blood cavity ratio in these patients did not exceed 0.2 in all subjects. Therefore, the cut-off maximal LV myocardium to blood cavity ratio of 2.0 was determined on this basis (maximal value of the maximal LV myocardium to blood cavity ratio in all individuals + [2 × intraobserver variability]).

All ^{11}C-PiB PET/CT images were quantified by a single experienced investigator blinded to all other findings of the patient. Additionally, the left myocardial wall was divided into 16 standardized segments according to the definition of the American Heart Association (10).

TABLE 1 ^{11}C-PiB PET/CT Results of Normal Control Subjects

			PiB PET/CT	
Patient #	Age, yrs	Sex	Maximal LV Myocardium-Blood Cavity Ratio	Mean LV Myocardium-Blood Cavity Ratio
1	80	M	1.40	1.17
2	59	M	1.60	1.11
3	65	F	1.31	1.11
4	54	F	1.22	1.01
5	56	F	1.39	0.88
6	51	F	1.17	1.10
7	59	F	1.00	0.94
8	58	F	1.27	1.10
9	37	M	0.88	0.76
10	55	M	1.49	1.26

The maximal SUV was defined as the maximal SUV in all of the VOIs analyzed. The mean SUV was defined as the mean SUV of the total voxels in the VOIs. The maximal/mean myocardium to blood cavity ratio was defined as the maximal/mean SUV of the myocardial VOIs divided by the mean SUV of the descending thoracic aorta VOIs.

CT = computed tomography; LV = left ventricular; PET = positron emission tomography; PiB = Pittsburgh B; SUV = standard uptake value; VOI = volume of interest.

CARDIAC MAGNETIC RESONANCE. The electrocardiogram-gated CMR images were taken using a standard 1.5-T scanner (Sonata Magnetom, Siemens Healthcare, Erlangen, Germany) or 3.0-T scanner (Trio, Siemens Healthcare) equipped with 6-channel phased-array receiver coils under the standard protocols. After taking initial scout images, steady-state free precession cine images were acquired under an adequate breath-hold for cine images. The imaging parameters for the cine images were: echo time 1.6 ms, repetition time 3.6 ms, flip angle 80°, matrix size 256 × 150, slice thickness 6 mm with 4 mm gap between adjacent slices, FOV 240 × 300 cm, and temporal resolution 32 ms. The LGE images were obtained after 10 min of intravenous gadolinium injection (0.1 mmol/kg Magnevist, Schering, Berlin, Germany) with 8 mm thickness, 2 mm interval. The imaging parameters for the LGE images were: slice thickness 8 mm, interslice gap 2 mm, echo time 42 ms, repetition time 9.1 ms, flip angle 13°, and in-plane resolution 1.4 × 1.9 mm. Inversion delay time varied according to the time to null the normal myocardium, especially because it is often difficult to determine the optimal inversion time in cardiac amyloidosis. All CMR images were analyzed by a single experienced investigator blinded to other findings of the patient.

STATISTICAL ANALYSIS. Continuous variables were presented as median (range) and number (percent) for categorical variables. The Mann-Whitney *U* test was used to compare continuous variables. The Fisher exact test was used to compare the differences in categorical data between the groups. The degree of correlation between the parameters was expressed with Spearman's ρ. A 2-tailed $p < 0.05$ was considered statistically significant.

RESULTS

A total of 22 patients were enrolled in this prospective pilot study, among whom 15 patients were diagnosed with cardiac amyloidosis using tissue confirmation by endomyocardial biopsy. Baseline clinical characteristics of these patients are summarized in Table 2. In the biopsy-proven cardiac amyloidosis group, the median age of the patients was 64 years, and 7 patients were male. Patients #1 to #15 were diagnosed with cardiac amyloidosis by positive Congo red staining and amyloid P staining on endomyocardial biopsy. The immunostaining of the endomyocardial biopsy samples were also matched with the serum free light chain assay results. All patients had AL amyloidosis, and there were no patients diagnosed with senile amyloidosis.

TABLE 2 Baseline Clinical Data and ^{11}C-PiB PET/CT Results of Each Study Participant

			Biopsy	PiB PET/CT							
Patient #	Age, yrs	Sex	Immunohisto-chemistry	Uptake	Maximal LV Myocardium-Blood Cavity Ratio	Mean LV Myocardium-Blood Cavity Ratio	ECG Low Voltage	Chemotherapy Before the Enrollment	Amyloid In Other Organs	ΔFLC (Before Chemotherapy)	ΔFLC (After Chemotherapy)
1	59	F	λ	Yes	3.86	2.27	Yes	No			
2	51	F	λ	Yes	13.94	4.94	Yes	No			
3	64	M	λ	Yes	19.92	8.92	Yes	No			
4	75	F	λ	Yes	18.03	10.70	Yes	No	Kidney		
5	60	F	κ	Yes	13.51	7.60	Yes	No	Kidney		
6	79	F	κ	Yes	3.63	1.69	Yes	No			
7	64	M	λ	Yes	4.26	2.28	Yes	No			
8	67	M	λ	Yes	15.89	9.41	Yes	No			
9	72	M	κ	Yes	7.27	3.73	Yes	No			
10	61	M	λ	Yes	2.29	0.99	No	MD#3→Auto-PBSCT		117 (27/144)	26 (17/43)
11	53	M	λ	Yes	3.81	1.08	Yes	MD#1		207 (28/235)	38 (3/41)
12	69	F	λ	Yes	2.39	1.17	No	MD#1		144 (16/160)	70 (32/102)
13	51	F	κ	Yes	2.05	1.19	Yes	TD#1		350 (606/256)	48 (50/2)
14	45	F	κ	No	1.69	0.95	Yes	No	Kidney		
15	62	M	λ	No	1.68	0.64	Yes	TD #6			35/1,151 (1,116)
16	79	M	Nonamyloid	No	0.92	0.87	Yes	No			
17	67	M	Nonamyloid	No	1.03	1.00	No	No			
18	76	F	Nonamyloid	No	0.97	0.96	No	No			
19	50	F	Nonamyloid	No	1.23	0.95	Yes	No	Kidney, liver		
20	77	F	Nonamyloid	No	0.89	0.76	No	No			
21	76	F	Nonamyloid	No	0.76	0.66	Yes	No			
22	73	M	Nonamyloid	No	1.11	0.98	Yes	No			

Individual clinical and ^{11}C-PiB PET/CT results of the study participants are listed. All patients were diagnosed with cardiac amyloidosis by positive Congo red and amyloid P immunohistochemical staining on endomyocardial biopsy. The immunostaining of the endomyocardial biopsy samples were also matched with the serum free light chain assay results. A cutoff value for positive versus negative ^{11}C-PiB PET/CT was defined as maximal myocardium-to-blood cavity ratio ≥2.0 on the basis of results of control subjects in Table 1. The difference between the involved and uninvolved free light chain levels is shown in the ΔFLC column with κ and λ levels in the parenthesis, respectively. #n indicates number of cycles of chemotherapy.

ECG = electrocardiogram; FLC = free light chain; MD = melphalan + dexamethasone; PBSCT = peripheral blood stem cell transplantation; TD = thalidomide + dexamethasone; other abbreviations as in Table 1.

A detailed description on the amyloidosis status of the enrolled patients is summarized in Table 2. There were 3 patients with concomitant renal amyloidosis in the biopsy-proven cardiac amyloidosis group in comparison with 1 patient having renal and hepatic amyloidosis in the no cardiac amyloidosis group. In addition, 5 patients (Patients #10 to #13, and #15) had undergone previous chemotherapy before the diagnosis of cardiac amyloidosis by endomyocardial biopsy. The serum free light chain assay results before and after the chemotherapy were available in 4 patients (Patients #10 to #13), all of whom showed a partial response of ≥50% decrease in the difference between involved and uninvolved free light chain levels (11). The initial serum free light chain assay result was unavailable in patient 15 because the patient was transferred from another hospital. No patients in the no cardiac amyloidosis group had undergone previous chemotherapy for monoclonal gammopathy.

The echocardiography data for all study participants are summarized in Table 3. There were no

TABLE 3 Echocardiography Data From All Study Participants

	Biopsy-Proven Cardiac Amyloidosis		
	Yes (n = 15)	No (n = 7)	p Value
LV end-diastolic dimension, mm	41.0 (33.0–49.0)	47.0 (38.0–55.0)	0.066
LV ejection fraction, %	56.0 (34.0–76.0)	64.5 (29.0–75.0)	0.731
Average wall thickness, mm	12.0 (9.0–17.0)	11.0 (9.5–16.0)	0.731
E velocity, m/s	0.80 (0.40–1.3)	0.65 (0.40–0.97)	0.368
e′ velocity at septal annulus, cm/s	4.3 (1.7–6.2)	3.6 (2.8–5.1)	0.569
LV hypertrophy	53.3 (8.0)	42.9 (3.0)	>0.999
Diastolic dysfunction grade			0.211
I	33.3 (5.0)	57.1 (4.0)	
II	33.3 (5.0)	42.9 (3.0)	
III	33.3 (5.0)	0.0 (0.0)	

Values are median (range) or % (n). The echocardiography was done at the time of enrollment. The e′ velocity was measured at the septal side of the mitral annulus.

LV = left ventricular.

differences in the echocardiographic parameters between the biopsy-proven cardiac amyloidosis group (Patients #1 to #15) and the no cardiac amyloidosis group (Patients #16 to #22), except for a marginal difference in the LV end-diastolic diameter (median 41.0 mm [range 33.0 to 49.0 mm] vs. 50.0 mm [range 38.0 to 55.0 mm], p = 0.066 with Mann-Whitney *U* test). Although grade III diastolic dysfunction was demonstrable only in patients in the biopsy-proven cardiac amyloidosis group, the overall degree of diastolic dysfunction was not significantly different between the 2 groups (p = 0.211).

Using the maximal LV myocardium to blood cavity SUV ratio of 2.0 for the cut-off of a positive ^{11}C-PiB PET/CT scan derived from 10 normal subjects, there was no patient with a false-positive ^{11}C-PiB PET/CT scan result in the no cardiac amyloidosis group. In contrast, there was 1 patient each in the chemotherapy-naïve (Patient #14) and the previous chemotherapy group (Patient #15) with false-negative ^{11}C-PiB PET/CT results (maximal LV myocardium to blood cavity ratio 1.69 and 1.68, respectively).

The maximal and the mean LV myocardium to blood cavity SUV ratios were significantly different

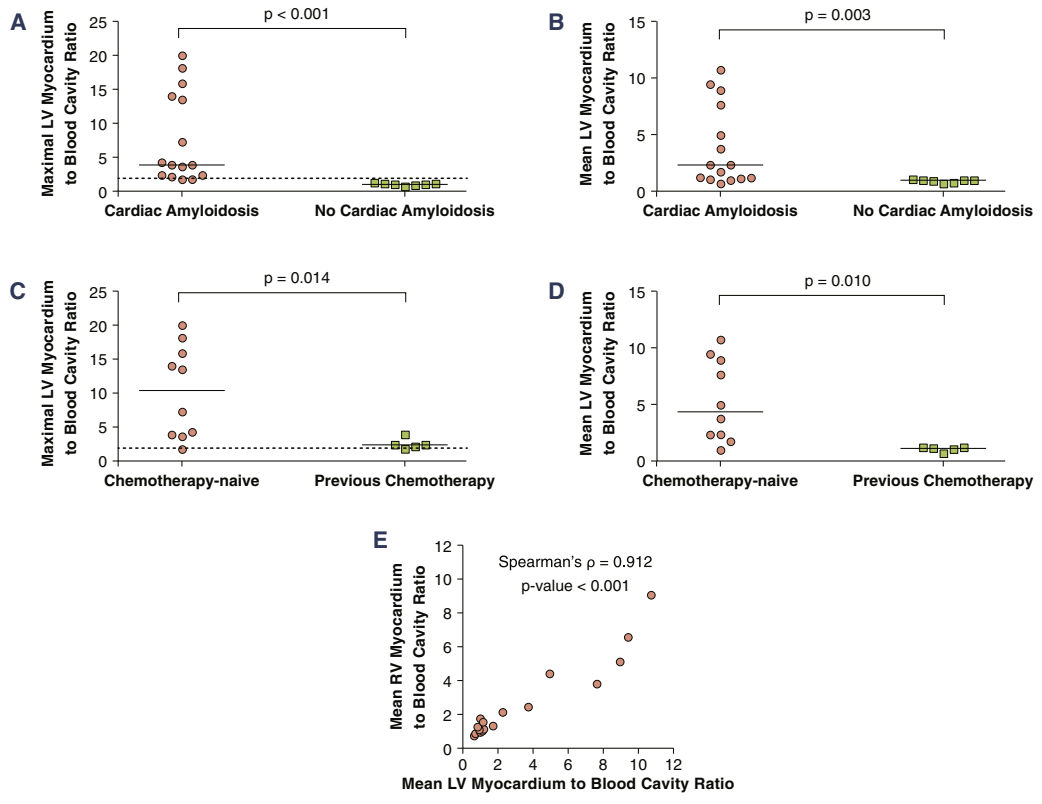

FIGURE 1 Comparison of the Standard Uptake Value Ratio of ^{11}C-PiB in the Study Participants

(A and B) The patients were grouped into those with endomyocardial biopsy-proven cardiac amyloidosis versus no cardiac amyloidosis. The maximal **(A)** and the mean **(B)** ^{11}C-Pittsburgh B (PiB) left ventricular (LV) myocardium to blood cavity standard uptake value (SUV) ratios were compared between the cardiac amyloidosis versus no cardiac amyloidosis groups. Note that there was no overlap of the maximal LV myocardium to blood cavity ratio in between patients with cardiac amyloidosis versus with no cardiac amyloidosis. A p value <0.001 for maximal LV myocardium to blood cavity SUV ratio and a p value of 0.003 for mean LV myocardium to blood cavity SUV ratio, both with Mann-Whitney *U* test. **(C and D)** The biopsy-proven cardiac amyloidosis patients were grouped into chemotherapy naïve patients and the patients who had undergone previous chemotherapy. The maximal **(C)** and the mean **(D)** ^{11}C-PiB LV myocardium to blood cavity SUV ratios were compared between the chemotherapy naïve and the previous chemotherapy patients. There was a p value of 0.014 for maximal LV myocardium to blood cavity SUV ratio and a p value of 0.010 for mean LV myocardium to blood cavity SUV ratio, both with Mann-Whitney *U* test. The **dotted line in A and C** denotes the cut-off value for a positive ^{11}C-PiB positron emission tomography/computed tomography. **Horizontal lines in A to D** indicate the median value of each group. **(E)** The correlation between mean right ventricular (RV) myocardium to blood cavity ratio versus mean LV myocardium to blood cavity ratio. Spearman's ρ = 0.912, p < 0.001.

between the cardiac amyloidosis group and the no cardiac amyloidosis group (median 3.86 [range 1.68 to 19.92] vs. 0.97 [range 0.76 to 1.23], $p < 0.001$ for maximal LV myocardium to blood cavity ratio [Figure 1A]; median 2.27 [range 0.64 to 10.70] vs. 0.95 [range 0.66 to 1.00], $p = 0.003$ for mean LV myocardium to blood cavity ratio [Figure 1B]). The maximal and the mean LV myocardium to blood cavity ratios were also significantly different between the chemotherapy naïve group and the previous chemotherapy group (median 10.39 [range 1.69 to 19.92] vs. 2.29 [range 1.68 to 3.81], $p = 0.014$ for maximal LV myocardium to blood cavity ratio [Figure 1C]; median 4.34 [range 0.95 to 10.70] vs. 1.08 [range 0.64 to 1.19], $p = 0.010$ for mean LV myocardium to blood cavity ratio [Figure 1D]). It was also notable that the degree of mean RV uptake was proportionate to the degree of mean LV uptake (Spearman's $\rho = 0.912$, $p < 0.001$ between mean LV vs. mean RV myocardium to blood cavity ratio) (Figure 1E).

Figure 2 shows the representative ^{11}C-PiB PET/CT scan and the corresponding LGE-CMR images of chemotherapy-naïve cardiac amyloidosis patients (Figures 2A and 2B), a cardiac amyloidosis patient who had undergone previous chemotherapy before ^{11}C-PiB PET/CT scan (Figure 2C), and a patient from the no cardiac amyloidosis group (Figure 2D). The ^{11}C-PiB uptake pattern was mainly diffuse and homogeneous at the LV as well as the RV (Figure 2A, patient 9). However, in some cases, the hot uptake was more striking at localized areas such as the septal and lateral segments (Figure 2B, patient 5). Although the maximal LV myocardium to blood cavity ratio was numerically higher in the cardiac amyloidosis patients who had undergone previous chemotherapy, the ^{11}C-PiB uptake was only marginally stronger in the cardiac amyloidosis patients who had undergone previous chemotherapy (Figure 2C) compared with the patients without cardiac amyloidosis (Figure 2D) on visual inspection.

The gadolinium-enhanced CMR was not performed in 3 patients in the ^{11}C-PiB PET/CT-negative group because of significant azotemia (creatinine clearance ≤30 ml/kg/min). Diverse patterns of LGE were noted in the patients, ranging from no LGE, to a more typical subendocardial ring enhancement, and to a

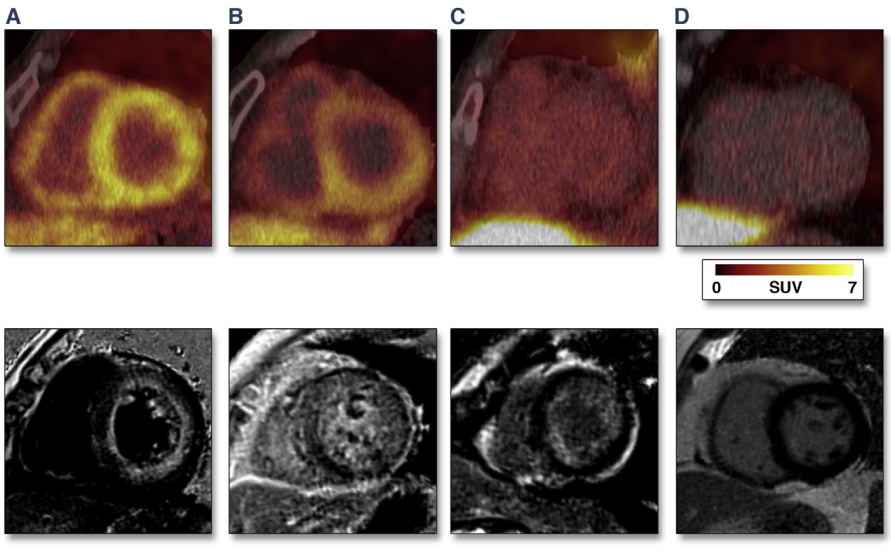

FIGURE 2 Representative ^{11}C-PiB PET/CT Images of the Study Participants

(A) Diffuse, homogeneous uptake pattern in patient 9. The uptake of ^{11}C-PiB was noted at both the LV and RV. Subendocardial ring enhancement pattern was noted at the late gadolinium enhancement (LGE)-cardiac magnetic resonance (CMR) image. **(B)** Heterogeneous uptake pattern in patient 5. Although there was uptake noted at other regions, the uptake of ^{11}C-PiB was more strongly positive at the inferoseptum and, to a lesser degree, at the lateral segment. Heterogeneous transmural enhancement pattern was present at the LGE-CMR image. **(C)** A representative ^{11}C-PiB positron emission tomography (PET)/computed tomography (CT) image of a patient who had undergone chemotherapy before ^{11}C-PiB PET/CT (Patient #12). The ^{11}C-PiB uptake was marginally elevated, and LGE-CMR demonstrated a subendocardial ring enhancement pattern. **(D)** A representative negative ^{11}C-PiB PET/CT scan image of a patient who did not have cardiac amyloidosis (Patient #18). The LGE-CMR image was also normal. Abbreviations as in Figure 1.

heterogeneous transmural LGE pattern (Table 4). Although only subendocardial ring enhancement pattern was noted in the previous chemotherapy group (Figure 2C), heterogeneous transmural LGE pattern was also seen (Figure 2B), as well as the subendocardial ring enhancement pattern in the chemotherapy naïve group (Figure 2A). There was 1 false-positive CMR case (Patient #16) in the biopsy-negative group. There was 1 false-negative CMR case (Patient #2) in the biopsy-positive group, which was correctly diagnosed with ^{11}C-PiB PET/CT (Figure 3), and 1 patient had both false-negative CMR and ^{11}C-PiB PET/CT (Patient #15) (Table 5).

Overall, the sensitivity and specificity of ^{11}C-PiB PET/CT for the diagnosis of cardiac amyloidosis was 0.87 (95% confidence interval [CI]: 0.58 to 0.98) and 1.00 (95% CI: 0.56 to 1.00), whereas for CMR it was 0.83 (95% CI: 0.51 to 0.97) and 0.85 (95% CI: 0.42 to 0.99). The diagnostic accuracy of ^{11}C-PiB PET/CT was 0.91, whereas for CMR it was 0.84.

DISCUSSION

Although the gold standard diagnostic tool for cardiac amyloidosis is endomyocardial biopsy (5), investigators have tried to assess this disease non-invasively with various imaging techniques. Although some molecular imaging-based methods have been successful (8,12), most of them have been unsuccessful for demonstrating amyloid deposits in the myocardium (13). The CMR has also been successful in the diagnosis of cardiac amyloidosis (14), but it may not be specific for amyloid deposits (15). Therefore, there is a clinical need to foster imaging-based diagnosis into clinical utility.

^{11}C-PiB has been used recently for early detection and for follow-up of Alzheimer's dementia (16), a disease characterized by accumulation of β-amyloid plaque in the brain parenchyme. It is a radioactive derivative of benzothiazole that binds with conformational dependence to any type of β-amyloid sheet structure (7). Indeed, this has been demonstrated in various mouse models (17) and in human autopsy studies of the brain (18). The clinical efficacy of the ^{11}C-PiB PET scan to predict the outcome in Alzheimer's dementia patients has recently been highlighted (16,19). These findings led us to investigate whether ^{11}C-PiB PET/CT may be a simple yet clinically useful method for detection of cardiac amyloidosis.

Although very preliminary and hypothetical at the current stage, the findings of the current study suggest that ^{11}C-PiB PET/CT results might be a useful surrogate marker of the status of cardiac amyloidosis. There have been several reports on the diagnosis of cardiac amyloidosis using simple methods, such as 12-lead electrocardiogram (20) and CMR (9,14,21), but none of these modalities is specific for the infiltration of amyloidogenic proteins itself. In this aspect, the ^{11}C-PiB PET/CT provides a unique experience for detection of the pathophysiological process itself in cardiac amyloidosis.

The concerns regarding the accuracy of each test for cardiac amyloidosis are reflected by the results of our cohort as well. Although a small population, approximately 80% of our patients with endomyocardial biopsy-proven amyloidosis displayed low voltage on 12-lead electrocardiogram. A previous paper reported a 50% to 60% diagnostic yield with the low voltage criteria (21). Therefore, although the suspicion of cardiac amyloidosis can be made with the low voltage criteria by 12-lead electrocardiogram (20), its diagnostic yield may not be sensitive enough. Increased LV wall thickness on echocardiography with evidence of systemic amyloidosis is assumed to be diagnostic of cardiac amyloidosis (5). However, approximately 40% of our patients did not display increased wall thickness on 2-dimensional echocardiography. Moreover, increased wall thickness on echocardiography is not pathognomonic of cardiac

TABLE 4 Baseline ^{11}C-PiB PET/CT and CMR Results From Each Study Participant

	PiB PET/CT	LGE-CMR
Patient #	Uptake	LGE pattern
1	Yes	Subendocardial ring LGE
2	Yes	Negative
3	Yes	Subendocardial ring LGE
4	Yes	Subendocardial ring LGE
5	Yes	Heterogeneous transmural LGE
6	Yes	Heterogeneous transmural LGE
7	Yes	Heterogeneous transmural LGE
8	Yes	Not done because of azotemia
9	Yes	Subendocardial ring LGE
10	Yes	Subendocardial ring LGE
11	Yes	Not done because of azotemia
12	Yes	Subendocardial ring LGE
13	Yes	Subendocardial ring LGE
14	No	Not done because of azotemia
15	No	Negative
16	No	Subendocardial ring LGE
17	No	Negative
18	No	Negative
19	No	Negative
20	No	Negative
21	No	Negative
22	No	Negative

CMR was done within 1 month of ^{11}C-PiB PET/CT. The pattern of LGE was classified as either negative, subendocardial ring type, or heterogeneous transmural type.

CMR = cardiac magnetic resonance; LGE = late gadolinium enhancement; other abbreviations as in Table 1.

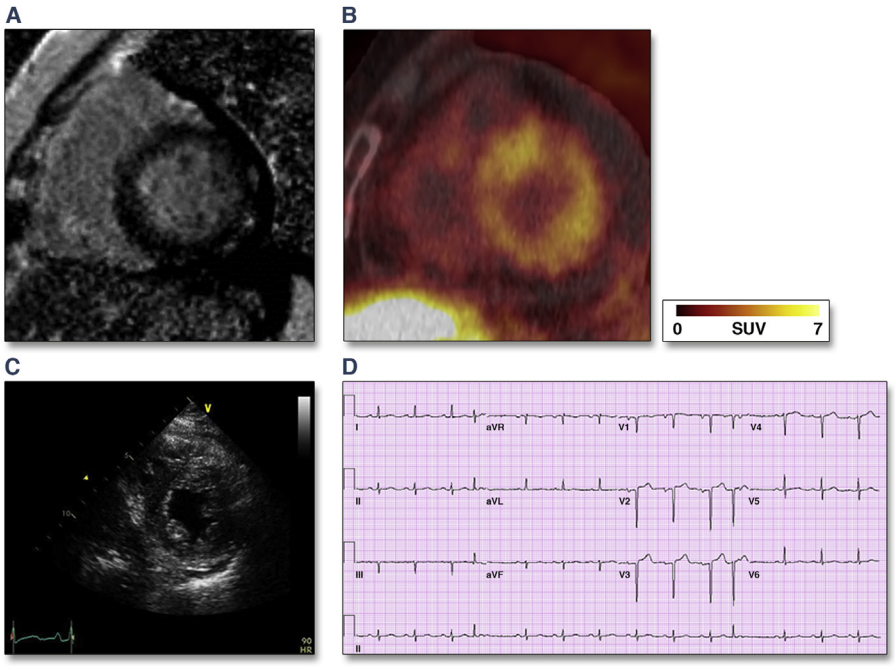

FIGURE 3 A Patient With False-Negative CMR Result That Was Correctly Diagnosed With ^{11}C-PiB PET/CT

(A) Although the CMR result did not show any late gadolinium enhancement (LGE) in the LV, the endomyocardial biopsy result was positive for cardiac amyloidosis (Patient #2). **(B)** The PET/CT showed strong uptake of ^{11}C-PiB in the myocardium. **(C)** The average wall thickness of the LV was 12 mm. **(D)** Low voltage in the limb leads was noted on 12-lead electrocardiogram. Abbreviations as in Figures 1 and 2.

amyloidosis, and other potential causes of LV hypertrophy must be excluded to diagnose cardiac amyloidosis on the basis of echocardiography findings (5). Even with the combination of both electrocardiogram and echocardiography findings, the diagnostic accuracy is barely 60% (21).

In line with this, the sensitivity and specificity of ^{11}C-PiB PET/CT show a potential clinical utility of PET/CT for diagnosis of cardiac amyloidosis. Even if taking into account the 2 false-negative ^{11}C-PiB PET/CT cases, the sensitivity and specificity of ^{11}C-PiB PET/CT were at least comparable to CMR for assessment of the amyloid deposits in cardiac amyloidosis, and these findings warrant further comparative studies of the accuracy between each test in a larger population. In addition, whereas the case of patient 2 demonstrated that ^{11}C-PiB PET/CT may be used complementarily to aid the diagnosis of cardiac amyloidosis (Figure 3), there was no case with false-negative ^{11}C-PiB PET/CT but with positive CMR results. In support of this, it has been reported in a previous study that the probability of a false-negative CMR may be approximately 12% in a biopsy-proven cardiac amyloidosis (21). Also, the case of Patient #8 demonstrates the unique opportunity of ^{11}C-PiB PET/CT for the diagnosis of cardiac amyloidosis in the setting of significant azotemia, a situation where contrast-enhanced CMR cannot be performed (22).

The true importance of our study is that quantitative assessment of amyloid deposit might be possible by using ^{11}C-PiB PET/CT in cardiac amyloidosis. The test results indicate that there is potential for the use

TABLE 5 Diagnostic Performance of Each Test in Patients Either With Biopsy-Proven Cardiac Amyloidosis or Without Evidence of Cardiac Amyloidosis on Endomyocardial Biopsy

		LGE-CMR	
		Yes	No
Biopsy positive			
PiB PET/CT uptake	Yes	10	1
	No	0	1
Biopsy negative			
PiB PET/CT uptake	Yes	0	0
	No	1	6

The diagnostic performance was compared between LGE-CMR and ^{11}C-PiB PET/CT according to the endomyocardial biopsy results, the gold standard.

Abbreviations as in Tables 1 and 4.

of ^{11}C-PiB PET/CT in assessing the disease burden, as shown by the significant difference of ^{11}C-PiB uptake between the chemotherapy naïve group and the previous chemotherapy group. Attempts to assess amyloid burden have also been made with CMR. As shown by the various LGE findings on CMR, a global transmural LGE pattern was associated with a more progressed state of cardiac amyloidosis (i.e., larger LV mass, worse LV ejection fraction, and worse functional capacity) compared with focal positive LGE pattern or negative LGE pattern (9). Patients with LGE were more likely to experience an adverse clinical event than patients without (21). However, the LGE pattern in cardiac amyloidosis is diverse even in a single cut of a given myocardium (9), making the classification obscure in some cases. In addition, gadolinium cannot be used in patients with azotemia (22), a finding that is not infrequently encountered in systemic amyloidosis, and there have been no data on whether LGE may reflect the amyloid burden after definite treatment. Furthermore, it may be virtually impossible to quantify LGE in a patient with a heterogeneous mix of diverse LGE patterns. In contrast, we were able to quantify the SUV of the myocardium using the ^{11}C-PiB PET/CT. Especially, considering that the majority of the patients who had undergone previous chemotherapy had at least a partial response to the treatment, the striking difference of ^{11}C-PiB uptake between the chemotherapy naïve group and the previous chemotherapy group suggests that the ^{11}C-PiB PET/CT results may reflect active deposition of amyloid protein in the myocardium. Further investigations in a larger population and follow-up scans may give further insight into the mechanism of the isotope uptake.

STUDY LIMITATIONS. First, the small number of patients makes some findings of our study difficult to generalize. Furthermore, all of our patients had AL amyloidosis, and whether our findings extend to other causes of cardiac amyloidosis, such as senile or hereditary amyloidosis, needs further observation. In this aspect, it is interesting to note that ^{11}C-PiB PET was valuable for the diagnosis of transthyretin-associated senile amyloidosis in a previous study (8). Second, we cannot provide data as to whether the myocardium to blood cavity ratio of ^{11}C-PiB is related to myocardial blood flow. However, all except 1 patient were void of any history of coronary artery disease, and a previous report has also demonstrated that the retention index of ^{11}C-PiB is unrelated to quantified myocardial blood flow (8). Third, we did not perform dynamic PET scans as in a previous study (8). However, we aimed to develop a relatively simple method that would be ready for clinical usage, an objective difficult to achieve with the kinetic model. Furthermore, the tissue to blood pool ratio tends to increase after 20 min post-injection (10), and we assumed that 30 min post-injection may be a sufficient time point to measure the tissue to blood pool ratio. Last, the current sample number may not be sufficient to make a reasonable comparison of the diagnostic performance between ^{11}C-PiB PET/CT and CMR.

CONCLUSIONS

We have shown in this pilot study that ^{11}C-PiB PET/CT may be valuable for noninvasive diagnosis of cardiac amyloidosis. Additionally, the significant difference of ^{11}C-PiB uptake between the chemotherapy naïve patients and the patients who had previous chemotherapy warrants further in-depth investigation into whether ^{11}C-PiB PET/CT can be used as a surrogate for active light chain deposition in the myocardium. If confirmed, the findings here may suggest an objective, noninvasive tool to assess the degree of cardiac involvement in systemic amyloidosis, which is valuable in deciding the treatment strategy.

ACKNOWLEDGMENT The authors would like to thank Hanna Choi, RN, for her help in management of the database.

REPRINT REQUESTS AND CORRESPONDENCE: Dr. Dae-Won Sohn, Cardiovascular Center, Seoul National University Hospital and Department of Internal Medicine, Seoul National University College of Medicine, Seoul 110-744, Korea. E-mail: dwsohn@snu.ac.kr.

REFERENCES

1. Merlini G, Bellotti V. Molecular mechanisms of amyloidosis. N Engl J Med 2003;349:583–96.

2. Falk RH, Comenzo RL, Skinner M. The systemic amyloidoses. N Engl J Med 1997;337:898–909.

3. Dubrey SW, Cha K, Anderson J, et al. The clinical features of immunoglobulin light-chain (AL) amyloidosis with heart involvement. QJM 1998;91:141–57.

4. Kyle RA, Gertz MA. Primary systemic amyloidosis: clinical and laboratory features in 474 cases. Semin Hematol 1995;32:45–59.

5. Gertz MA, Comenzo R, Falk RH, et al. Definition of organ involvement and treatment response in immunoglobulin light chain amyloidosis (AL): a consensus opinion from the 10th International Symposium on Amyloid and Amyloidosis, Tours, France, 18-22 April 2004. Am J Hematol 2005;79:319–28.

6. Klunk WE, Engler H, Nordberg A, et al. Imaging brain amyloid in Alzheimer's disease with Pittsburgh Compound-B. Ann Neurol 2004;55:306–19.

7. Biancalana M, Koide S. Molecular mechanism of Thioflavin-T binding to amyloid fibrils. Biochim Biophys Acta 2010;1804:1405–12.

8. Antoni G, Lubberink M, Estrada S, et al. In vivo visualization of amyloid deposits in the heart with 11C-PIB and PET. J Nucl Med 2013;54:213–20.

9. Syed IS, Glockner JF, Feng D, et al. Role of cardiac magnetic resonance imaging in the detection of cardiac amyloidosis. J Am Coll Cardiol Img 2010;3:155–64.

10. Price JC, Klunk WE, Lopresti BJ, et al. Kinetic modeling of amyloid binding in humans using PET imaging and Pittsburgh Compound-B. J Cereb Blood Flow Metab 2005;25:1528–47.

11. Lachmann HJ, Gallimore R, Gillmore JD, et al. Outcome in systemic AL amyloidosis in relation to changes in concentration of circulating free immunoglobulin light chains following chemotherapy. Br J Haematol 2003;122:78–84.

12. Dorbala S, Vangala D, Semer J, et al. Imaging cardiac amyloidosis: a pilot study using (18)F-florbetapir positron emission tomography. Eur J Nucl Med Mol Imaging 2014;41:1652–62.

13. Glaudemans AW, Slart RH, Zeebregts CJ, et al. Nuclear imaging in cardiac amyloidosis. Eur J Nucl Med Mol Imaging 2009;36:702–14.

14. Maceira AM, Joshi J, Prasad SK, et al. Cardiovascular magnetic resonance in cardiac amyloidosis. Circulation 2005;111:186–93.

15. Mahrholdt H, Wagner A, Judd RM, Sechtem U, Kim RJ. Delayed enhancement cardiovascular magnetic resonance assessment of non-ischaemic cardiomyopathies. Eur Heart J 2005;26:1461–74.

16. Bateman RJ, Xiong C, Benzinger TL, et al. Clinical and biomarker changes in dominantly inherited Alzheimer's disease. N Engl J Med 2012;367:795–804.

17. Bacskai BJ, Hickey GA, Skoch J, et al. Four-dimensional multiphoton imaging of brain entry, amyloid binding, and clearance of an amyloid-beta ligand in transgenic mice. Proc Natl Acad Sci U S A 2003;100:12462–7.

18. Burack MA, Hartlein J, Flores HP, Taylor-Reinwald L, Perlmutter JS, Cairns NJ. In vivo amyloid imaging in autopsy-confirmed Parkinson disease with dementia. Neurology 2010;74:77–84.

19. Dore V, Villemagne VL, Bourgeat P, et al. Cross-sectional and longitudinal analysis of the relationship between Abeta deposition, cortical thickness, and memory in cognitively unimpaired individuals and in Alzheimer disease. JAMA Neurol 2013;70:903–11.

20. Carroll JD, Gaasch WH, McAdam KP. Amyloid cardiomyopathy: characterization by a distinctive voltage/mass relation. Am J Cardiol 1982;49:9–13.

21. Austin BA, Tang WH, Rodriguez ER, et al. Delayed hyper-enhancement magnetic resonance imaging provides incremental diagnostic and prognostic utility in suspected cardiac amyloidosis. J Am Coll Cardiol Img 2009;2:1369–77.

22. Rydahl C, Thomsen HS, Marckmann P. High prevalence of nephrogenic systemic fibrosis in chronic renal failure patients exposed to gadodiamide, a gadolinium-containing magnetic resonance contrast agent. Invest Radiol 2008;43:141–4.

KEY WORDS cardiac amyloidosis, cardiac magnetic resonance, echocardiography, Pittsburgh B compound, positron emission tomography

APPENDIX For a detailed version of the Methods section, please see the online version of this article.